

PAPER • OPEN ACCESS

Effect of annealing on the room temperature luminescence of coumarin 106 in PVA films

To cite this article: Emma Alexander *et al* 2024 *Methods Appl. Fluoresc.* **12** 015005

View the [article online](#) for updates and enhancements.

You may also like

- [Room Temperature Phosphorescence of 5,6-Benzoquinoline](#)
Jose Chavez, Luca Ceresa, Emma Kitchner et al.
- [Temperature dependence of the phosphorescence and of the thermally activated delayed fluorescence of \$^{12}\text{C}_{70}\$ and \$^{13}\text{C}_{70}\$ in amorphous polymer matrices. Is a second triplet involved?](#)
Tiago Palmeira, Alexander Fedorov and Mário N Berberan-Santos
- [Ex situ calibration technique for simultaneous velocity and temperature measurements inside water droplets using temperature-sensitive particles](#)
Qian Zhou, Nejdet Erkan and Koji Okamoto



WORLD LEADING
MOLECULAR
SPECTROSCOPY SOLUTIONS



edinst.com

Methods and Applications in Fluorescence



PAPER

Effect of annealing on the room temperature luminescence of coumarin 106 in PVA films

OPEN ACCESS

RECEIVED
12 July 2023

REVISED
26 September 2023

ACCEPTED FOR PUBLICATION
25 October 2023

PUBLISHED
2 November 2023

Emma Alexander* , Luca Ceresa , Danh Pham , Zygmunt Gryczynski and Ignacy Gryczynski

Department of Physics and Astronomy, Texas Christian University, Fort Worth, TX, 76129, United States of America

* Author to whom any correspondence should be addressed.

E-mail: e.l.alexander@tcu.edu

Keywords: room-temperature phosphorescence, coumarin 106, annealing

Original content from this work may be used under the terms of the [Creative Commons Attribution 4.0 licence](https://creativecommons.org/licenses/by/4.0/).

Any further distribution of this work must maintain attribution to the author(s) and the title of the work, journal citation and DOI.



Abstract

We studied the effect of annealing on the luminescence of Coumarin 106 (C106) in poly (vinyl alcohol) films (PVA films). The samples and reference polymer films were treated at temperatures between 100 °C and 150 °C (212 F and 302 F) for various times. After cooling and smoothing, the samples and references were measured at room temperature. We observed that the PVA polymer (reference films) changes its optical properties with annealing at higher temperatures, affecting the baselines in absorption and the backgrounds in emission measurements. This requires precise background subtractions and control of the signal-to-noise ratio. Whereas the fluorescence intensity of C106 in PVA films modestly decreases with annealing, the phosphorescence depends dramatically and progressively increases by many folds. The fluorescence quantum yields and lifetimes decrease with the annealing, which suggests an increase in the non-radiative processes in the singlet excited state S_1 . The increase in the phosphorescence intensities results from increased intersystem crossing (ISC), which also decreases fluorescence. We also studied the effect of annealing on phosphorescence with the directly excited triplet state of C106. In this case, two processes are affected by annealing, $S_0 \rightarrow T_1$ absorption and $T_1 \rightarrow S_0$ phosphorescence. The long-wavelength excitation (475 nm) avoids PVA polymer excitation. The phosphorescence lifetime decreases with annealing while the phosphorescence intensity increases. These changes suggest that the radiative rate of $T_1 \rightarrow S_0$ increases with annealing.

1. Introduction

A laser dye Coumarin 106 (C106) (also known as Coumarin 478) was synthesized and introduced in the middle of the 1970 s [1]. The molecule of C106 is rigid and has a fairly planar structure [2]. This smartly designed dye is reasonably soluble in polar solvents. It is also solvent sensitive because its electric dipole increases substantially upon excitation [3], enabling its use as a chemo-sensor [4]. Recently, we discovered that C106 shows efficient room temperature phosphorescence (RTP) when embedded in poly (vinyl alcohol) (PVA) films [5].

Moreover, we also reported that the phosphorescence of C106 in PVA films can be excited outside the absorption band with a long-wavelength (475 nm) light. In this case, the C106 triplet state has been populated directly through $S_0 \rightarrow T_1$ absorption. RTP has

recently gained interest because of possible applications in encryption, decryption [6, 7], and counterfeiting [8]. An efficient RTP has been observed in metal-organic hybrids [9–11]. RTP of xanthene derivatives crystals has been proposed for imaging [12]. Any practical application of RTP will benefit from stronger emission signals. The rigidity of the medium plays an important role in phosphorescence emission. Therefore, most reports on RTP are on crystals, sol-gels, and doped polymers. An interesting effect of increased phosphorescence is reported by co-assembling biphenyl and naphthalene derivatives in low-density PVA [13].

Efficient, practical methods of enhancing the properties of the medium and RTP signal are freeze-thaw and/or annealing [14]. Annealing (thermal treatment) has been applied to PVA doped with silver nanoparticles [15] and carbon films and dots [16, 17].

Recently several reports appeared on annealing PVA polymers doped with carbon nanodots [18–20]. The impact of the fabrication process on the RTP of small-molecule-doped polymers has been described [19]. All these reports suggest using temperatures below the PVA polymer melting point (about 200 °C). In addition to efficient water removal from the PVA film following annealing, structural changes to the polymer structure can appear [21, 22, 37], changing polymer properties. For example, an annealing treatment of 135 °C increases the PVA fiber stiffness by 80% [22]. Intrigued, we decided to check the effect of annealing on C106-doped PVA luminescence (absorption, fluorescence, and phosphorescence). We will apply annealing temperatures up to 150 °C (for different amounts of time) for C106 doped PVA films and to the control samples-PVA films only with comparable thickness.

2. Materials and methods

The Coumarin 106 used is laser grade (purity $\geq 98\%$) and is from Kodak (now Estman-Kodak). Before use, C106 was recrystallized from a methanol-water solution. Poly (vinyl alcohol) [MW 130,000, 98% hydrolyzed] was obtained from Millipore Sigma [Sigma Aldrich].

2.1. Preparation of poly(vinyl alcohol) films

PVA films are prepared from a 10% (w/w) solution of PVA and deionized water. The PVA bulk solution was made in a 500 ml Erlenmeyer flask and was heated/steered at 95 °C until the solution became clear and had a honey-like consistency. The stock solutions of C106 were made in 20 ml of 10% (w/w) PVA solution, mixed, and then transferred to an 8.5 cm diameter Petri dish. Blank PVA films were made for background signal corrections. Drying the C106 films in the Petri dishes took about a week. After drying, the films were removed from the Petri dishes, and their thicknesses were measured with a caliper. The average thickness of each film was 0.02 cm. The estimated concentrations of C106 in PVA films were between 0.5–2 mM.

2.2. Annealing

Annealing of films has been done with a gravity convection lab oven. The temperature was stabilized with ± 2 °C accuracy. The samples were loaded into the preheated oven.

2.3. Absorption measurements

The Varian Cary 60 UV–vis Spectrophotometer (Agilent Technologies, Inc) was used to measure the absorption spectra at room temperature. Each film was measured multiple times, and the absorbances were averaged. Blank PVA was used for baseline corrections unless specified otherwise.

2.4. Fluorescence measurements

Fluorescence measurements were conducted on a Varian Cary Eclipse spectrofluorometer (Agilent Technologies, Inc). Front-face fluorescence measurements were made with a custom-made attachment with a UV grid polarizer on the excitation and a plastic sheet polarizer on the emission [23]. Fluorescence lifetimes were measured with FluoTime200 (Picoquant, GmbH), and the data were analyzed with the FluoFit program (Picoquant, GmbH, Version 4.4).

2.5. Phosphorescence measurements

The Varian Cary Eclipse instrument has a mode allowing for time-gated phosphorescence detection. Time-gating mode eliminates the short-lived emission component (Raman scattering, scattering, and fluorescence backgrounds). Unless specified in the figures, the parameters used in this mode were: Total Decay Time: 0.5 s, Number of flashes: 5, Delay Time: 0.2 ms, and Gate Time: 5 ms. More details can be found in the Phosphorescence Measurement section of [5]. Phosphorescence excitation and emission anisotropies were calculated from measured polarized intensity components I_{VV} and I_{VH} as:

$$r = \frac{I_{VV} - I_{VH} * G}{I_{VV} + 2I_{VH} * G} \quad (1)$$

I_{VV} and I_{VH} are phosphorescence intensities measured with a vertically polarized excitation and observed through vertically or horizontally oriented polarizers, respectively. G (G-Factor) has been used to correct the uneven transmissions of I_{VV} and I_{VH} through the detection path. The G-factor was measured for the front-face configuration described in [23].

2.6. Phosphorescence lifetime measurements

For lifetime measurements, we used a Varian Cary Eclipse spectrofluorometer (Agilent Technologies, Inc.) which is equipped with a lifetime function for a sub-second time scale. The gating parameters were the same as for phosphorescence spectra measurements and focused on specific excitation and emission wavelengths, as depicted in the figures. The collected time-dependent intensities were fitted to a multi-exponential model:

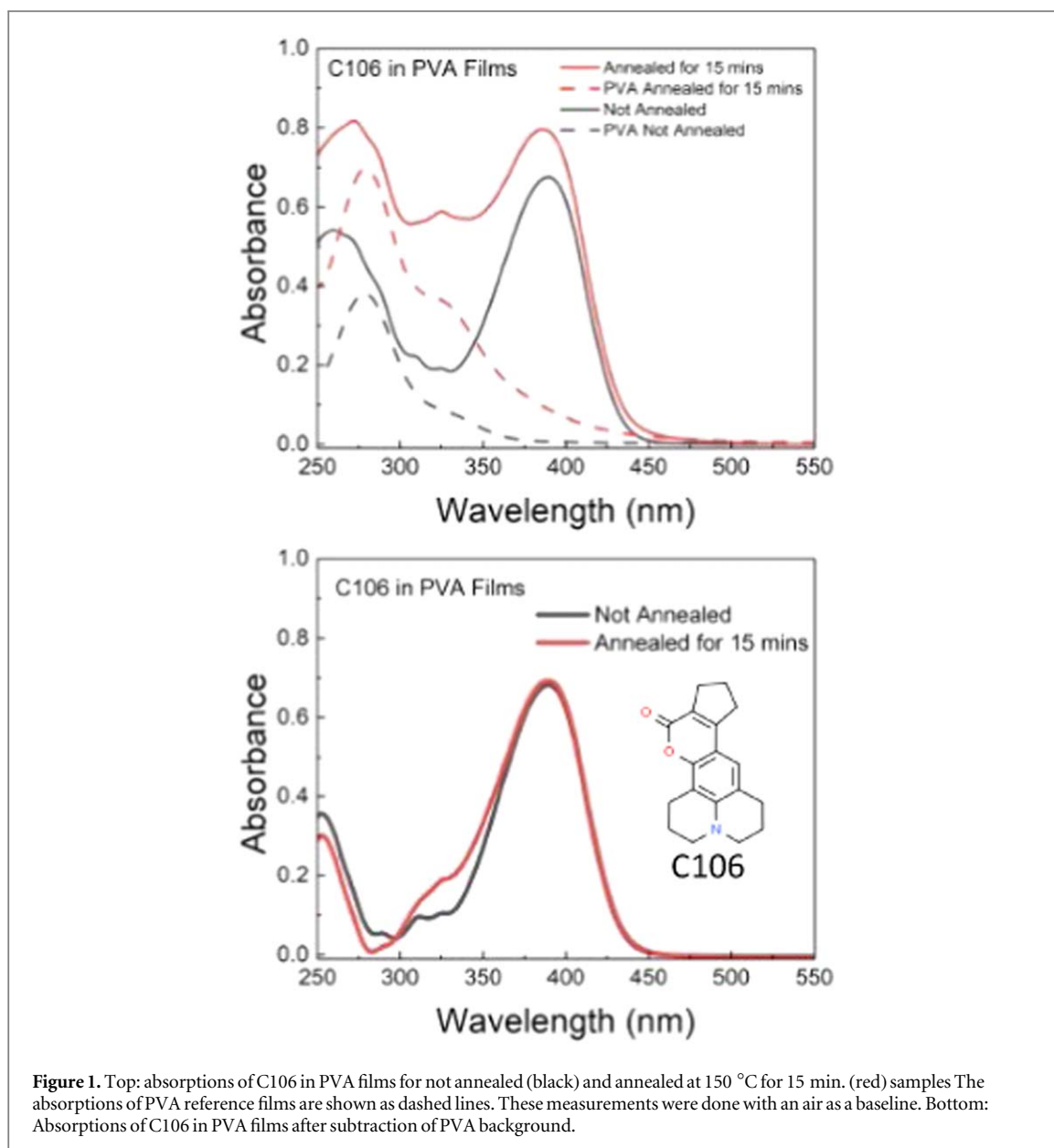
$$I(t) = I_0 \sum_i \alpha_i e^{-t/\tau_i} \quad (2)$$

Where the α_i term represents the amplitude for the i th intensity decay component at a time t_0 and τ_i represents the lifetime of that component.

For calculating intensity ($\langle \tau \rangle_{\text{int}}$) and amplitude ($\langle \tau \rangle_{\text{amp}}$) average decays, the following formulas were used:

$$\langle \tau \rangle_{\text{int}} = \sum f_i \tau_i \quad (3)$$

$$\langle \tau \rangle_{\text{amp}} = \sum \alpha_i \tau_i \quad (4)$$



$$f_i = \frac{\alpha_i \tau_i}{\sum \alpha_i \tau_i} \quad (5)$$

Equations (1)–(5) describe multi-exponential approximation of the emission intensity decay with the analysis based on least-square method, see more details in [23–25]:

The applicability of appropriate average values has been described in [26].

3. Results and discussion

We targeted a 0.6 absorbance of C106 in PVA with a film thickness of about 200 microns, knowing that volume decreases about 12–13 fold for 10% PVA (130,000 MW) upon drying [23]. Solutions in Petri dishes were dried at room temperature on a leveled surface. After the PVA samples were completely dry, films were pulled from the dishes and cut into strips. The thicknesses of the film strips were measured with a

caliper. The film strips were arranged in pairs of sample-reference (PVA filmed doped with C106 and PVA only film) with the same thicknesses.

First, we applied the annealing temperature of 150 °C for 15 min to C106 doped PVA film and to the control sample-PVA film with similar thickness. After the annealed samples were cooled down, the measurements were done at room temperature. Keep in mind that all temperatures used on annealing in our experiments are above the PVA film glass transition temperature of 85 °C, [27].

3.1. Effect of annealing on C106 in PVA film absorption

Absorbances of C106 in PVA Films (not annealed and annealed at 150 °C for 15 min) are shown in figure 1. Clearly, the absorbance of the annealed sample increased at shorter wavelengths in UV. However, the increase is clearly a result of changed PVA absorption.

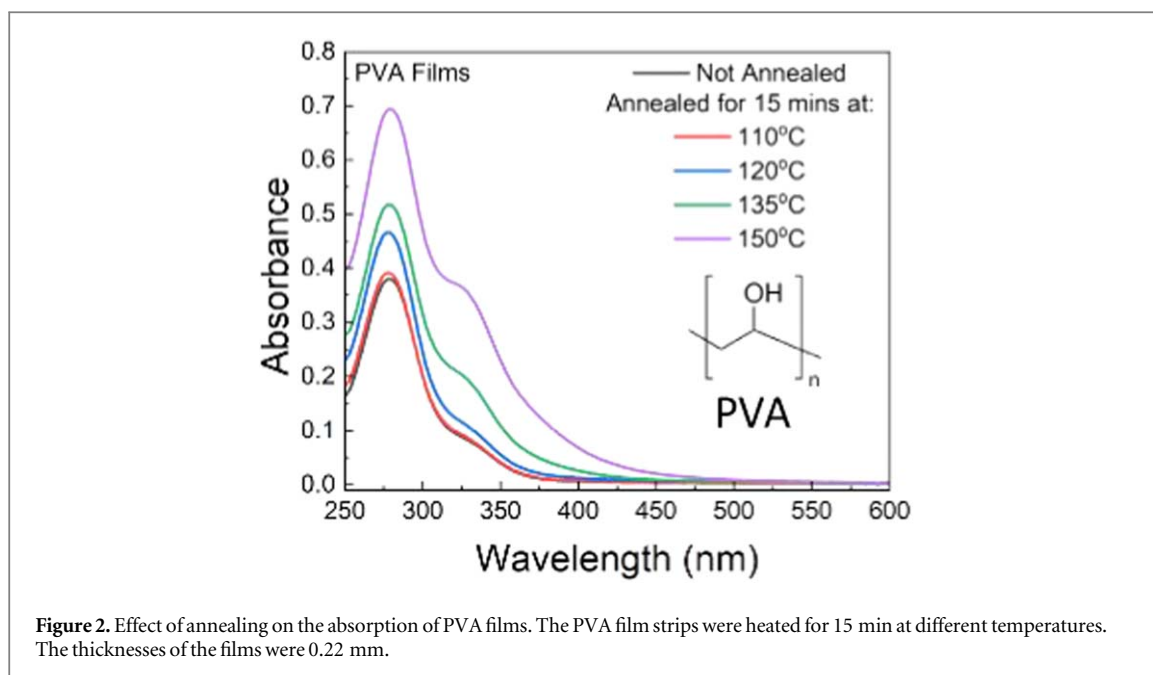


Figure 2. Effect of annealing on the absorption of PVA films. The PVA film strips were heated for 15 min at different temperatures. The thicknesses of the films were 0.22 mm.

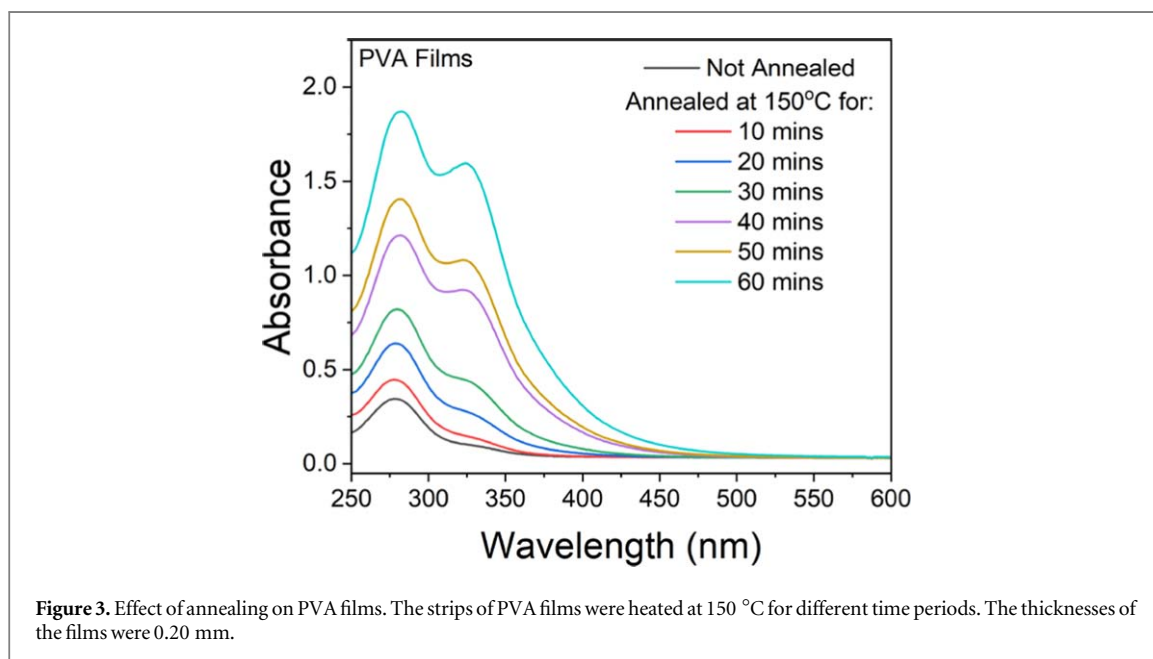


Figure 3. Effect of annealing on PVA films. The strips of PVA films were heated at 150 °C for different time periods. The thicknesses of the films were 0.20 mm.

PVA absorption can seriously affect the samples absorbing light in the UV spectral region. Therefore, we decided to look more into PVA absorbance changes upon annealing.

3.2. Effect of annealing on PVA films

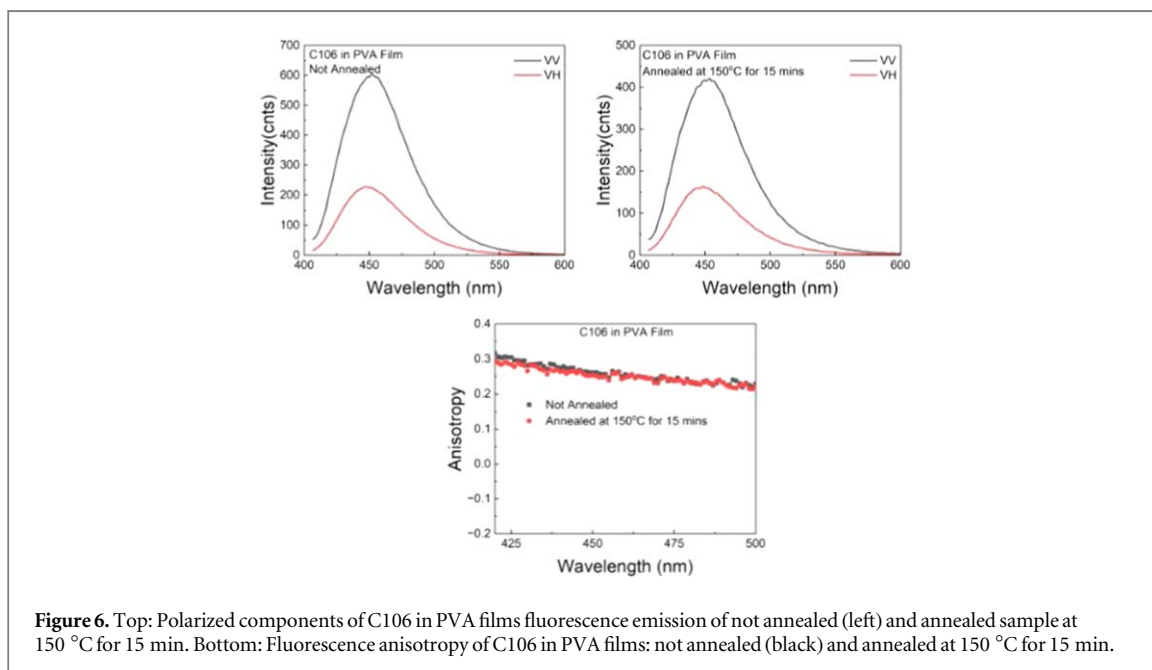
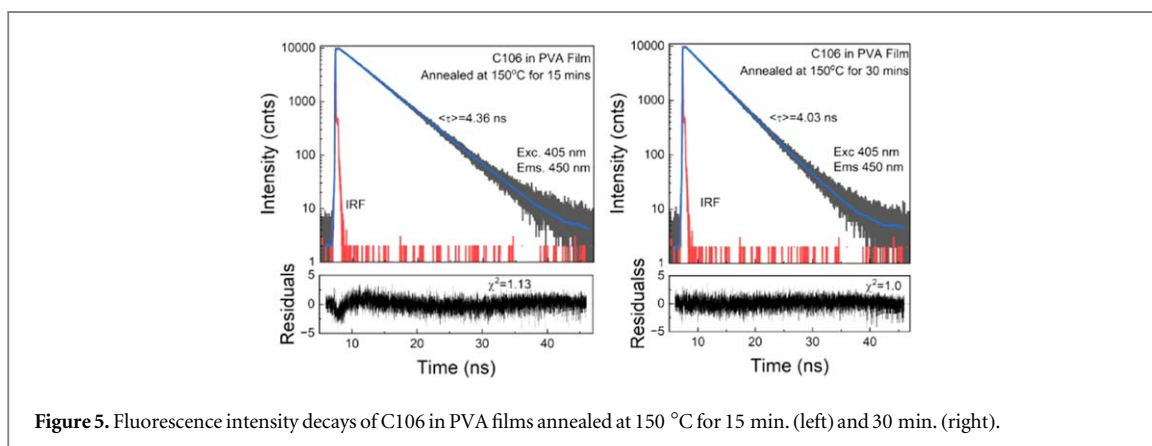
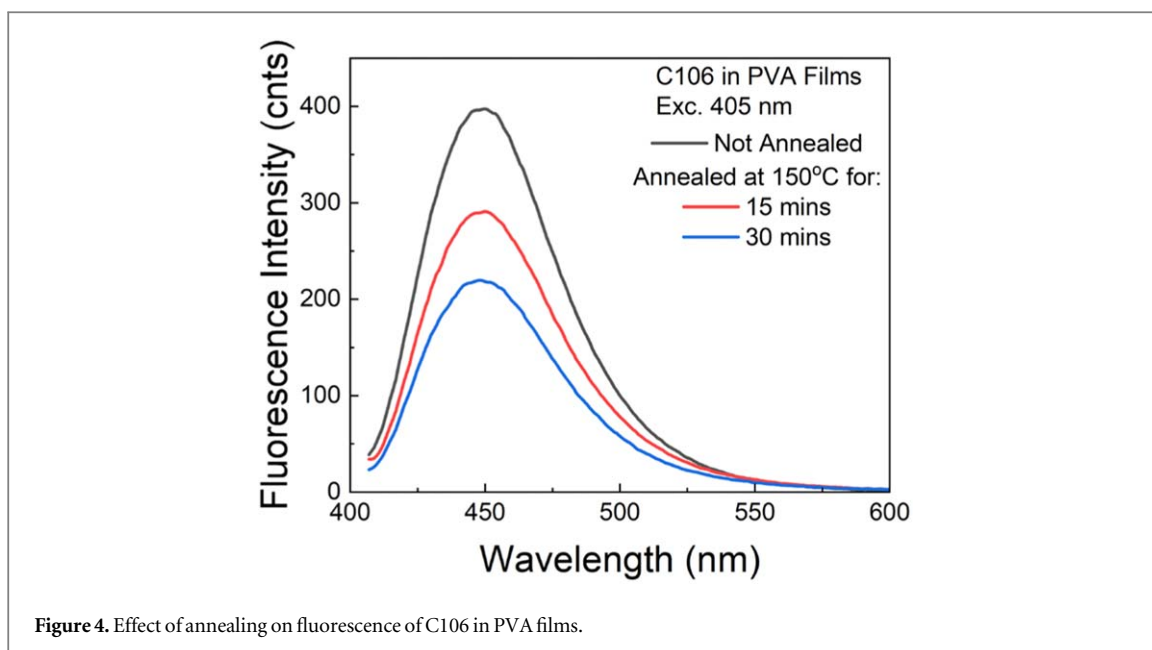
Absorbances of PVA annealed at different temperatures for 15 min are shown in figure 2. Interestingly, annealing at 110 °C practically does not change the PVA absorption. Another series of film strips were annealed at 150 °C for different periods, up to one hour, see figure 3.

Evidently, anyone using UV excitation must consider the PVA absorption for both inner-filter effects (absorption of the excitation light and absorption of fluorescence emission). Fortunately, the long

wavelength absorption of C106 is not strongly overlapped with PVA absorption. The differences in the PVA Annealed films versus the not annealed films can be found in *Supplementary Materials* (SM), figure SM1.

3.3. Effect of annealing on C106 in PVA films fluorescence spectra

While the absorption of C106 in PVA films does not depend significantly on annealing, fluorescence emission decreases for annealed samples substantially, see figure 4. Annealing at 150 °C for 30 min results in an almost 50% decrease in fluorescence intensity. Progressive fluorescence intensity changes at different temperatures are shown in figure SM2.



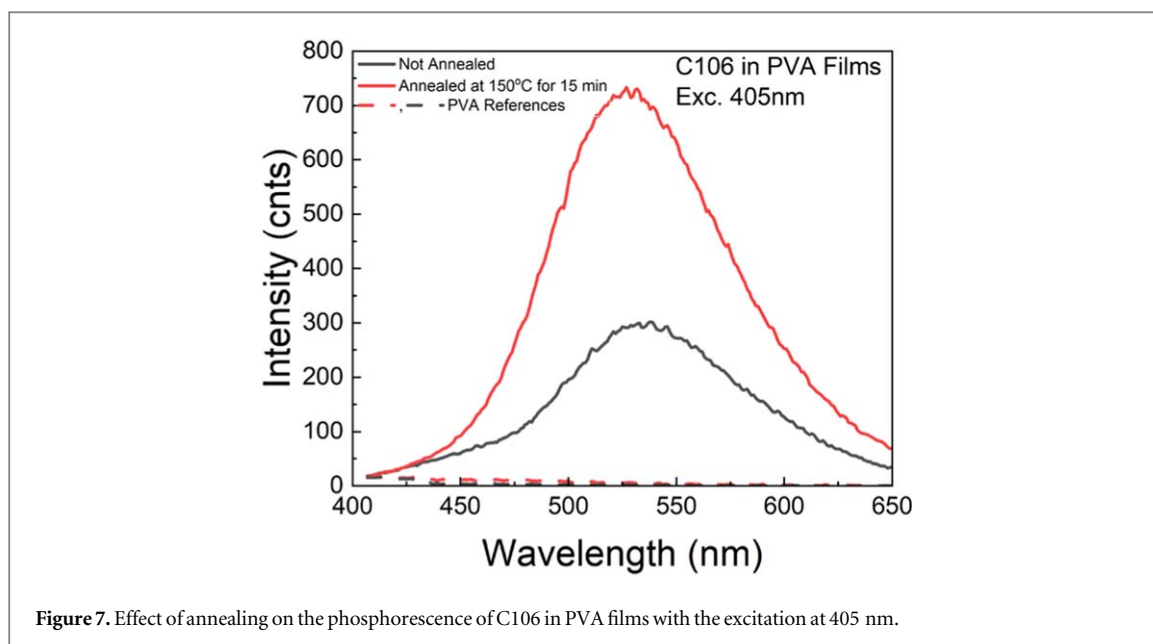


Figure 7. Effect of annealing on the phosphorescence of C106 in PVA films with the excitation at 405 nm.

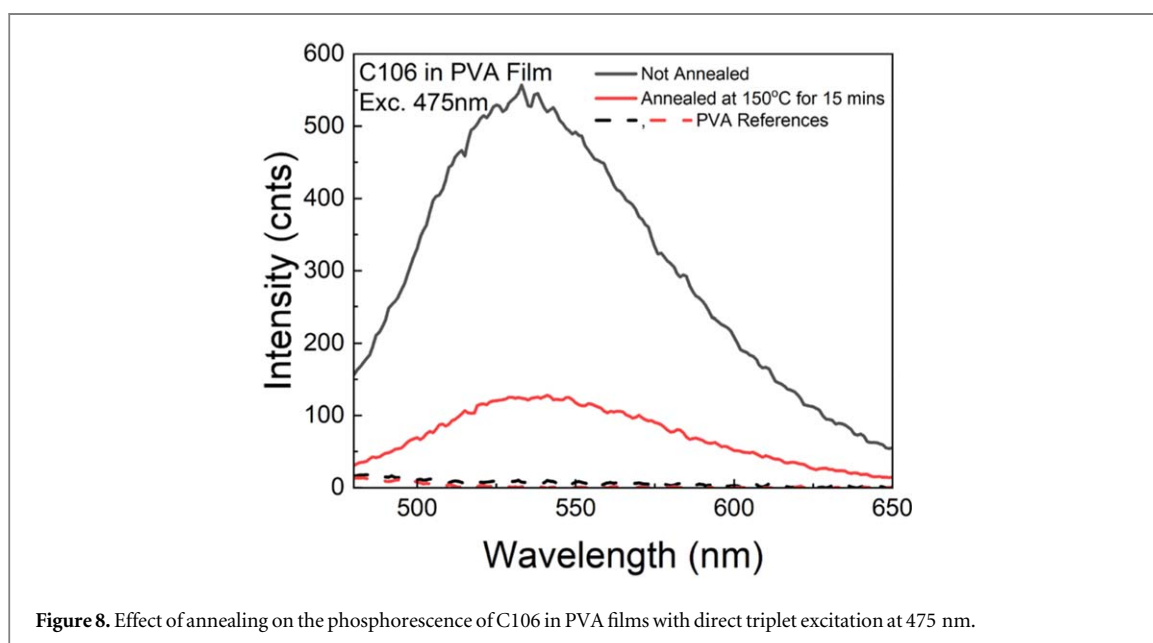


Figure 8. Effect of annealing on the phosphorescence of C106 in PVA films with direct triplet excitation at 475 nm.

3.4. Effect of annealing C106 in PVA films fluorescence lifetimes

The not annealed C106 in PVA film has a fluorescence lifetime of about 5 ns [5]. Lifetimes of C106 in PVA samples progressively decrease with the increase in annealing time, see figure 5. Both the fluorescence intensity and lifetime measurements suggest that deactivation processes increase in annealed samples (changes in absorptions are insignificant).

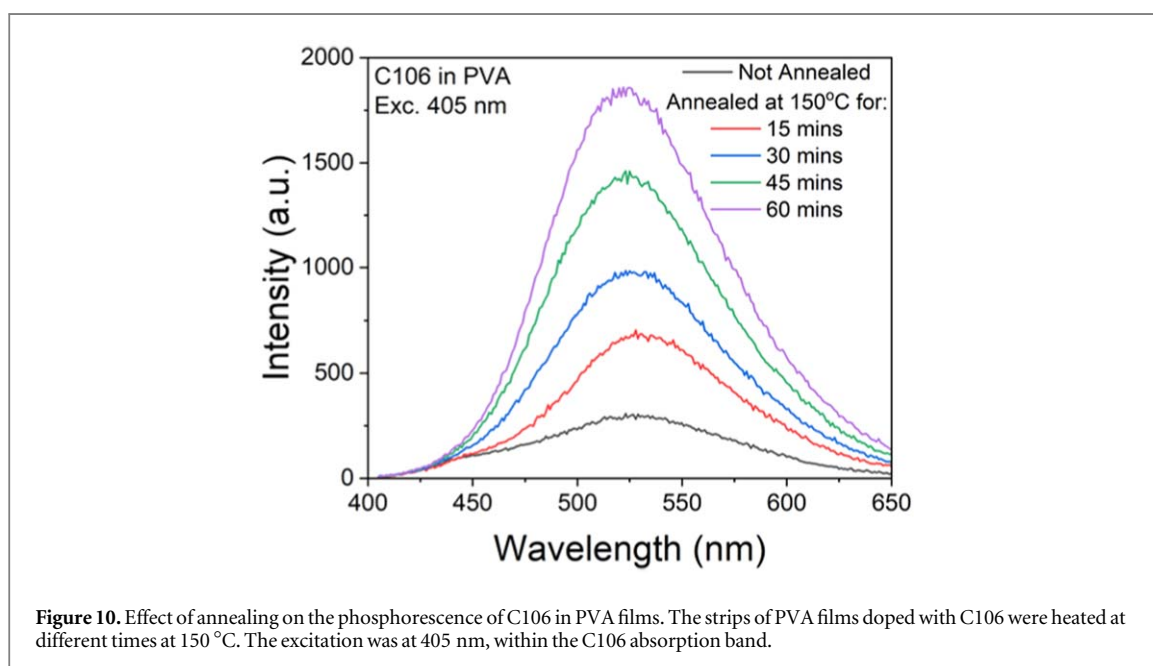
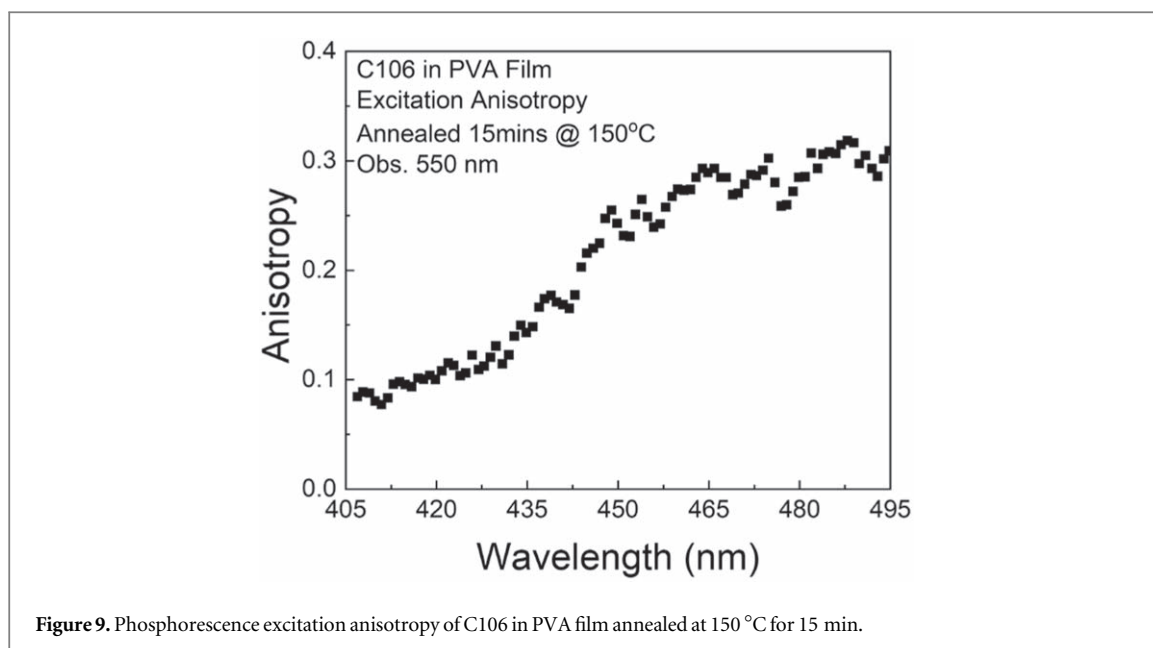
3.5. Effect of annealing C106 in PVA fluorescence anisotropy

We wondered if annealing affects fluorescence anisotropy. The measurements of fluorescence emission anisotropies for not annealed and annealed samples are shown in figure 6. Evidently, anisotropies are not affected by the annealing process. However, it must be

noted that PVA strips cannot be placed between rigid surfaces (like glass slides) and squeezed in annealing, and the cooling cannot be rapid. Not carefully performing the annealing process may result in PVA residual crystallization, and these areas become optically active (rotate the plane of light polarization); see figure SM3 in *Supplementary Materials*.

3.6. Effect of annealing on C106 in PVA phosphorescence

Based on other annealing reports described in the Introduction section, we were optimistic that C106 would show an improved RTP. Indeed, the phosphorescence intensity of annealed C106 in PVA film shows a significant increase, see figure 7. The measurement was done with 405 nm excitation within the absorption band. The 405 nm excitation results in a residual



delayed fluorescence (DF) already observed in [5]. Contrary to phosphorescence, the DF does not depend strongly on annealing. The phosphorescence backgrounds from both annealed, and non-annealed samples (dashed lines) are negligible.

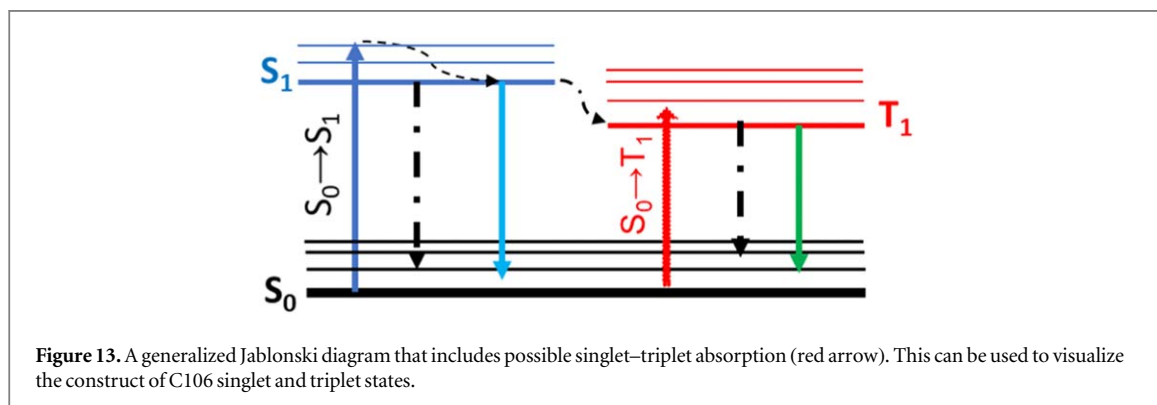
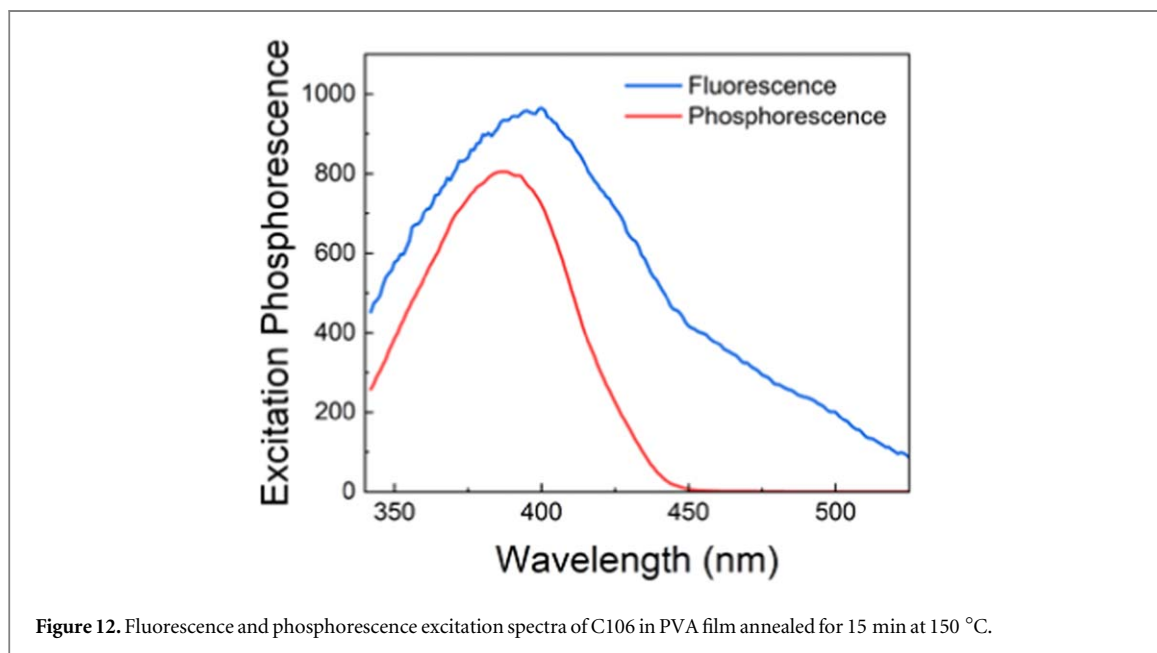
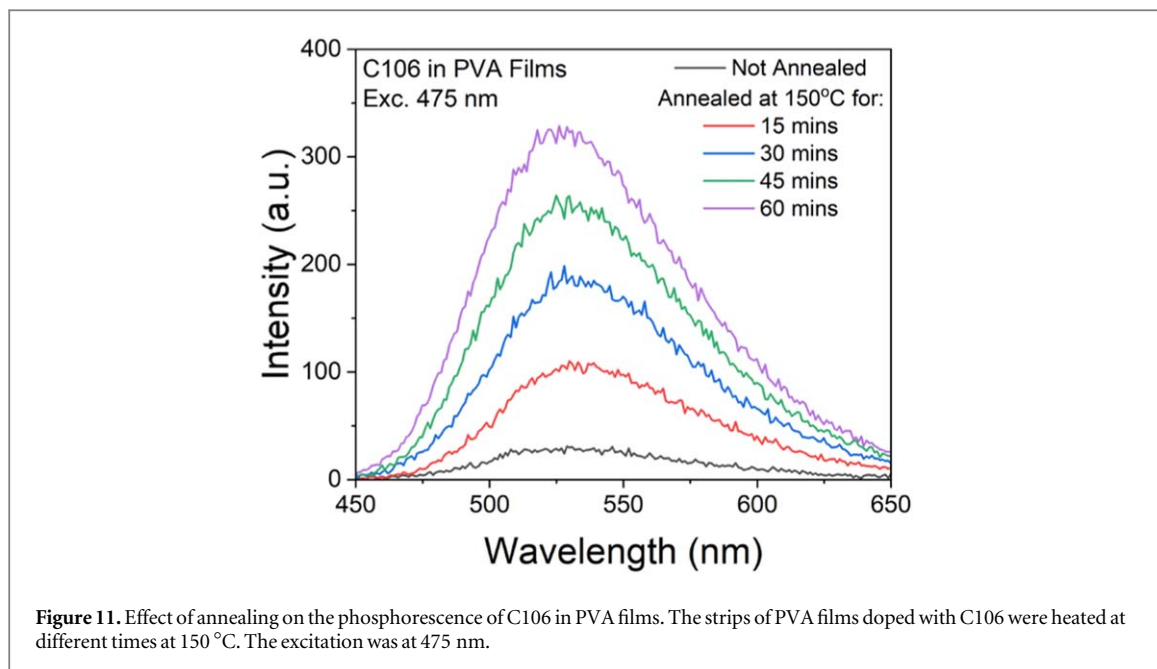
For a few years, we studied the RTP of different organic molecules embedded in PVA polymer excited directly to triplet states at longer wavelengths [5, 28–34]. The long-wavelength excitation (475 nm) of C106 in PVA samples is shown in figure 8. Compared to 405 nm excitation, the effect is even stronger. Such long-wavelength excitation of RTP results not only in the lower background but also in higher anisotropy, see figure 9. The excitation to S_1 state results in very low/negative phosphorescence anisotropy because T_1 state (populated by the inter-system crossing process)

is orthogonal to the singlet. In the case of direct triplet state excitation, the phosphorescence anisotropy is high, just like for fluorescence.

All of the measurements mentioned above were done with the same pair of not annealed/annealed samples and their references.

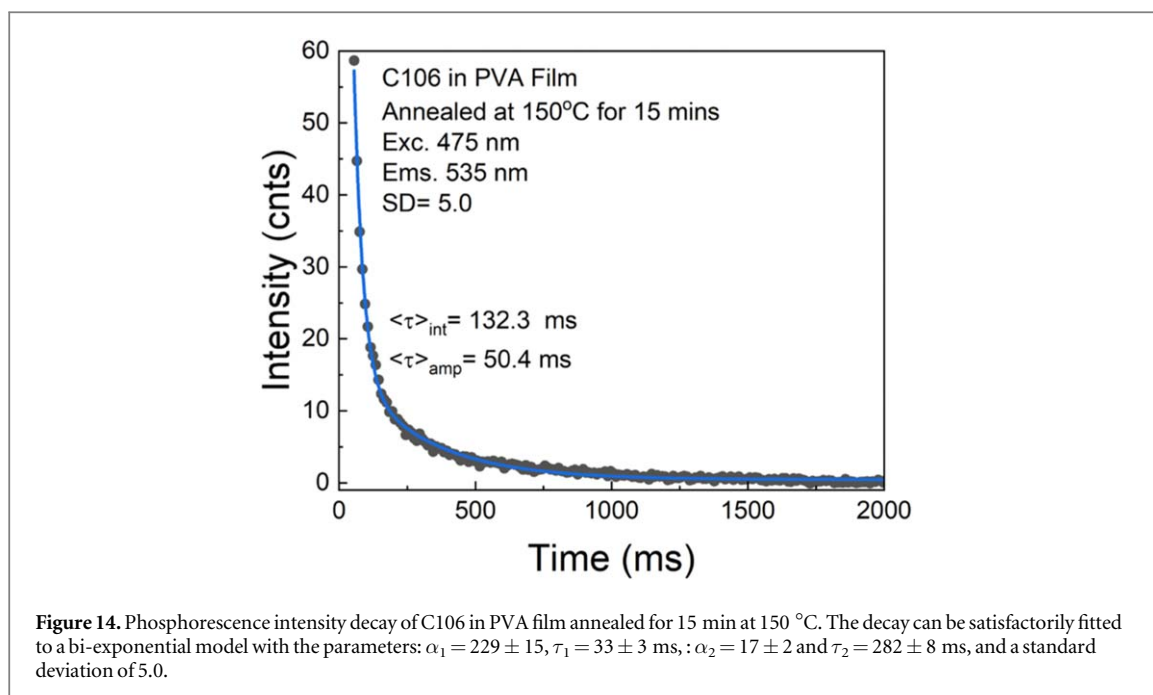
The strong effect of annealing increasing the phosphorescence of the samples encouraged us to study this as a function of different annealing times. The effect exceeded our expectations; see figures 10 and 11. Many fold enhancements have been observed for 405 nm and 475 nm excitations.

At 405 nm excitation, the phosphorescence spectra have been corrected for inner filter effects due to PVA absorptions as described in [23, 35, 36].



No corrections for inner filter effects were needed with 475 nm excitation; see PVA absorptions in figure 3.

3.7. Effect of annealing on C106 in PVA discussion
 What is the reason for the enhancement upon annealing? First, the remaining water molecules are removed



from the polymer. Second, reaching glass temperature, polymer molecules can more tightly surround the doped molecules. This will result in stronger interactions between the doped molecule and the polymer chain, which may activate spin-orbit perturbations. This will also explain that some molecules show a stronger phosphorescence enhancement when their shapes fit better to the polymer chain arrangement.

The phosphorescence excitation spectrum of annealed C106 in PVA film differs from the fluorescence excitation spectrum, see figure 12. Both spectra measured in fluorescence (blue) and phosphorescence (red) modes were observed at 560 nm with the same slits on excitation and observation paths. Above 450 nm, fluorescence (singlet state) was not excited. At longer wavelengths, the triplet state T_1 of C106 has been directly excited. We believe the transition $S_0 \rightarrow T_1$ is missed in the commonly accepted Jablonski diagram, see figure 13, [23–25]. Furthermore, we calculated the difference between S_1 and T_1 to about 3500 cm^{-1} . The calculation was based on the positions of emissions maxima, 450 nm for fluorescence and 535 nm for phosphorescence.

The average phosphorescence lifetime of C106 in PVA film at 475 nm excitation is about 370 ms, slightly longer than with UV excitation (360 ms) [5]. However, with annealing, it is shorter, 132 ± 5 ms, see figure 14. At the same time, the phosphorescence intensity increases proportionally, see figure 8. A simultaneous increase in intensity and decrease in a lifetime has been observed in metal-enhanced fluorescence [25] and explained by a modification of the radiative decay rate (called radiative decay engineering). In the case of annealing, we believe that the radiative rate increases also due to stronger spin-orbit interactions. The

decrease in the non-radiative rate would result in an increased lifetime.

Finally, how to use annealing with UV excitations where absorption of PVA might be high? Looking at figure 2, the annealing at 110 °C practically does not change PVA absorption. With fresh samples, we repeated the experiments (absorption, fluorescence, and phosphorescence) using annealing at 110 °C for 30 min, see Supplementary Materials, Figures SM4-SM8. About 100% enhancement in phosphorescence intensity can be achieved without altering PVA absorption.

4. Conclusions

The measurements presented above clearly show the possibility to enhance by annealing the phosphorescence intensities of C106 in PVA polymer by several fold, without altering their spectral or polarization properties. We believe that this may significantly influence the possible RTP applications of this and other dyes. Can this effect universally apply to all organic dyes? Although it is too early to answer this question, and more experimental data are needed, we observed some enhancement upon annealing for several other dyes like Coumarin120 or DAPI. However, we did not observe such enhancement for Coumarin 540 or Benzophenones.

Regardless, the possibility of achieving effective RTP with long-wavelength excitation simplifies these measurements and provides potential improvements. More powerful excitations can be obtained from blue/green lasers, and detector efficiency is significantly increase in the blue/green range. And the use of longer wavelength excitations results in lower background

and unwanted scattering, allowing for more signal to be detected.

Acknowledgments

We dedicate this paper to Professor Julian Borejdo for the occasion of his 75th birthday.

The authors have declared that no conflicting interests exist.

Z Gryczynski acknowledges support from 'Tex' Moncrief Jr and TCU College of Science and Engineering.

Data availability statement

The data cannot be made publicly available upon publication because they are not available in a format that is sufficiently accessible or reusable by other researchers. The data that support the findings of this study are available upon reasonable request from the authors.

ORCID iDs

Emma Alexander  <https://orcid.org/0000-0002-9226-2432>

Luca Ceresa  <https://orcid.org/0000-0001-8771-496X>

Danh Pham  <https://orcid.org/0000-0003-0274-9640>

References

- [1] Reynolds GA and Drexhage KH 1975 New coumarin dyes with rigidized structure for flashlamp-pumped *Optics. Comm.* **13** 222–5
- [2] Honda T, Fujii I, Hirayama N, Aoyama N and Miike A 1996 Organic compounds: coumarin 106, C18H19NO2 *Acta Cryst. C* **52** 364–5
- [3] Patil SK, Wari MN, Panicker CY and Inamdar SR 2014 Determination of ground and excited state dipole moments of dipolar laser dyes by solvatochromic shift method *Spectrochim. Acta, Part A* **123** 117–26
- [4] Cao D, Liu Z, Verwilt P, Koo S, Jangjili P, Kim JS and Lin W 2019 Coumarin-based small-molecule fluorescent chemosensors *Chem. Rev.* **119** 10403–519
- [5] Alexander E, Chavez J, Ceresa L, Seung M, Pham D, Gryczynski Z and Gryczynski I 2023 *Dyes Pigm.* **217** 111389
- [6] Su Y, Phua SZF, Li Y, Zhou X, Jana D, Liu G, Lim WQ, Ong WK, Yang C and Zhao Y 2018 Ultralong room temperature phosphorescence for amorphous organic materials toward confidential information encryption and decryption *Sci. Adv.* **4** eaas9732
- [7] Sun W, Shi Z, Xia Z and Lu C 2023 Visible-light-excited long-lived organic room-temperature phosphorescence of phenanthroline derivatives in PVA matrix by H-bonding interaction for security applications *Mat. Today Chem.* **27** 101297
- [8] Gao R, Yan D, Evans DG and Duan X 2017 Layer-by-layer assembly of long-afterglow self-supporting thin films with dual-stimuli-responsive phosphorescence and antiforgery applications *Nano Res.* **10** 3606
- [9] Zhou B, Qi Z and Yan D 2022 Highly efficient and direct ultralong all-phosphorescence from metal-organic framework photonic glasses *Angew. Chem. Int. Ed.* **61** e202208735
- [10] Yang X and Yan D 2016 Strongly Enhanced long-lived persistent room temperature phosphorescence based on the formation of metal-organic hybrids *Adv. Optical Mater.* **4** 897–905
- [11] Gao R, Kodaimati MS and Yan D 2021 Recent advances in persistent luminescence on molecular hybrid materials *Chem. Soc. Rev.* **50** 5564
- [12] Liao Q et al 2020 Dimethylxanthene derivatives with room-temperature phosphorescence: substituent effects and emissive properties *Angew. Chem. Int. Ed.* **59** 9946–51
- [13] Wu H, Gu L, Baryshnikov GV, Wang H, Minaev BF, Agren H and Zhao Y 2020 Molecular Phosphorescence in polymer matrix with reversible sensitivity. *Appl. Mater. and Interfaces*
- [14] Fukumori T and Nakaoki T 2013 Significant improvement of mechanical properties for polyvinyl alcohol film prepared from freeze/thaw cycled gel *Open J. Polym. Mater.* **3** 38808
- [15] Deb S and Sarkar D 2018 Effect of annealing temperature on optical properties of silver-PVA nanocomposite *Optik.* **157** 1115–21
- [16] Wang S and Komvopoulos K 2020 Structure evolution during deposition and thermal annealing of amorphous carbon ultrathin films investigated by molecular dynamics simulations *Sci. Rep.* **10** 8089
- [17] Wei X, Yang J, Hu L, Cao Y, Lai J, Cao F, Gu J and Cao X 2021 Recent advances in room temperature phosphorescent carbon dots: preparation, mechanism, and applications *J. Mater. Chem. C* **9** 4425
- [18] Bao X, Ushakova EV, Liu E, Zhou Z, Li D, Zhou D, Qu S and Rogach AL 2019 On–Off switching of the phosphorescence signal in a carbon dot/polyvinyl alcohol composite for multiple data encryption *Nanoscale.* **30** 14250–5
- [19] Zheng C, Tao S and Yang B 2023 Polymer-structure-induced room temperature Phosphorescence of carbon dot materials *Small Struct.* **4** 2200327
- [20] Tian Z and Li D 2018 Multilevel data encryption using thermal-treatment controlled room temperature phosphorescence of carbon dot/polyvinylalcohol composites *Adv. Sci.* **18** 1–71800795
- [21] Thomas D and Cebe P 2017 Self-nucleation and crystallization of polyvinyl alcohol *J. Therm. Anal. And Calorimetry* **127** 885–94
- [22] Wong KK, Zinke-Almang M and Wan W 2010 Effect of annealing on aqueous stability and elastic modulus of electrospun poly(vinyl alcohol) fibers *J. Mater. Sci.* **45** 2456–65
- [23] Gryczynski Z and Gryczynski I 2020 *Practical Fluorescence Spectroscopy* (Boca Raton, Florida: CRS Press, Taylor and Francis Group) 1st edn
- [24] Valeur B 2001 *Molecular Fluorescence: Principles and Applications* (Wiley-VCH Verlag GmbH)
- [25] Lakowicz JR 2006 *Principles of Fluorescence Spectroscopy* (Springer)
- [26] Sillen A and Engelborghs Y 1998 The correct use of 'average' fluorescence parameters *Photochem Photobiol* **67** 475–86
- [27] Tsiptsias C, Fardis D, Ntampou X, Tsivintzelis I and Panayiotou C 2023 Thermal behavior of poly(vinyl alcohol) in the form of physically crosslinked film. *Polymers* **15** 1843
- [28] Gryczynski Z, Kimball J, Fudala R, Chavez J, Ceresa L, Szabelski M, Borejdo J and Gryczynski I 2020 Photophysical properties of 2-Phenylindole in Poly(vinyl alcohol) film at room temperature. Enhanced phosphorescence anisotropy with direct triplet state excitation *Methods. Appl. Fluoresc.* **8** 014008
- [29] Chavez J, Ceresa L, Kitchner E, Kimball J, Shtoyko T, Fudala R, Borejdo J, Gryczynski Z and Gryczynski I 2020 On the possibility of direct triplet state excitation of indole *JPPB: Biology.* **208** 111897
- [30] Chavez J, Kimball J, Ceresa L, Kitchner E, Shtoyko T, Fudala R, Borejdo J, Gryczynski Z and Gryczynski I 2021 Luminescence properties of 5-bromindole in PVA films at room

- temperature: direct triplet state excitation *J. Luminescence* **230** 117724
- [31] Chavez J, Ceresa L, Reeks J M, Strzhemechny Y M, Kimball J, Kitchner E, Gryczynski Z and Gryczynski I 2022 Direct excitation of tryptophan phosphorescence, a new method triplet states investigation *Methods Appl. Fluoresc.* **10** 025001
- [32] Chavez J, Ceresa L, Kimball J, Kitchner E, Gryczynski Z and Gryczynski I 2022 Room temperature luminescence of 5-chloroindole *J. Mol. Liquids* **360** 119482
- [33] Chavez J, Ceresa L, Kitchner E, Pham D, Gryczynski Z and Gryczynski I 2023 Room temperature phosphorescence of 5,6-benzoquinoline *Methods Appl. Fluoresc.* **11** 025003
- [34] Chavez J, Ceresa L, Kitchner E, Pham D, Gryczynski Z and Gryczynski I 2023 Room temperature phosphorescence of 2-aminopyridine with direct triplet state excitation *Spectrochim. Acta - A: Mol. Biomol.* **295** 122640
- [35] Kimball J, Chavez J, Ceresa L, Kitchner E, Nurekeyev Z, Doan H, Szabelski M, Borejdo J, Gryczynski I and Gryczynski Z 2020 On the origin and correction for inner filter effects in fluorescence Part I: primary inner filter effect-the proper approach for sample absorbance correction *Methods Appl. Fluoresc.* **8** 033002
- [36] Ceresa L, Kimball J, Chavez J, Kitchner E, Nurekeyev Z, Doan H, Borejdo J, Gryczynski I and Gryczynski Z 2021 On the origin and correction for inner filter effects in fluorescence. part ii: secondary inner filter effect -the proper use of front-face configuration for highly absorbing and scattering samples *Methods Appl. Fluorescence.* **9** 035005
- [37] Thomas H, Haase K, Achenbach T, Bärschneider T, Kirch A, Talnack F, Mannsfeld S C B and Reineke S 2022 *Front. Phys.* **10** 1–8841413